Molecular Genetics and Metabolism 105 (2012) 91–102

Contents lists available at SciVerse ScienceDirect

Molecular Genetics and Metabolism

journal homepage: www.elsevier.com/locate/ymgme

Initial experience in the treatment of inherited mitochondrial disease with EPI-743

Gregory M. Enns [a,*], Stephen L. Kinsman [b], Susan L. Perlman [c], Kenneth M. Spicer [d], Jose E. Abdenur [e], Bruce H. Cohen [f], Akiko Amagata [g], Adam Barnes [g], Viktoria Kheifets [g], William D. Shrader [g], Martin Thoolen [g], Francis Blankenberg [h], Guy Miller [g,i]

[a] Department of Pediatrics, Division of Medical Genetics, Lucile Packard Children's Hospital, Stanford University, Stanford, CA 94305-5208, USA
[b] Division of Neurosciences, Medical University of South Carolina, Charleston, SC 29425, USA
[c] Department of Neurology, David Geffen School of Medicine, University of California, Los Angeles, CA 90095, USA
[d] Department of Radiology and Radiological Science, Medical University of South Carolina, Charleston, SC 29425, USA
[e] Department of Pediatrics, Division of Metabolic Disorders, CHOC Children's Hospital, Orange County, CA 92868, USA
[f] Department of Neurology, NeuroDevelopmental Science Center, Akron Children's Hospital, Akron, OH 44308, USA
[g] Edison Pharmaceuticals, 350 North Bernardo Avenue, Mountain View, CA 94043, USA
[h] Department of Radiology, Division of Pediatric Radiology, Lucile Packard Children's Hospital, Stanford, CA 94305, USA
[i] Department of Anesthesiology, Critical Care Medicine, Stanford University, Stanford, CA 94305, USA

ARTICLE INFO

Article history:
Received 22 September 2011
Received in revised form 17 October 2011
Accepted 17 October 2011
Available online 21 October 2011

Keywords:
α-Tocotrienol quinone
Leigh syndrome
Polymerase γ deficiency
MELAS
Mitochondrial DNA deletion syndrome
Friedreich ataxia

ABSTRACT

Inherited mitochondrial respiratory chain disorders are progressive, life-threatening conditions for which there are limited supportive treatment options and no approved drugs. Because of this unmet medical need, as well as the implication of mitochondrial dysfunction as a contributor to more common age-related and neurodegenerative disorders, mitochondrial diseases represent an important therapeutic target. Thirteen children and one adult with genetically-confirmed mitochondrial disease (polymerase γ deficiency, $n=4$; Leigh syndrome, $n=4$; MELAS, $n=3$; mtDNA deletion syndrome, $n=2$; Friedreich ataxia, $n=1$) at risk for progressing to end-of-life care within 90 days were treated with EPI-743, a novel *para*-benzoquinone therapeutic, in a subject controlled, open-label study. Serial measures of safety and efficacy were obtained that included biochemical, neurological, quality-of-life, and brain redox assessments using technetium-99m-hexamethylpropyleneamine oxime (HMPAO) single photon emission computed tomography (SPECT) radionuclide imaging. Twelve patients treated with EPI-743 have survived; one polymerase γ deficiency patient died after developing pneumonia and one patient with Surf-1 deficiency died after completion of the protocol. Of the 12 survivors, 11 demonstrated clinical improvement, with 3 showing partial relapse, and 10 of the survivors also had an improvement in quality-of-life scores at the end of the 13-week emergency treatment protocol. HMPAO SPECT scans correlated with clinical response; increased regional and whole brain HMPAO uptake was noted in the clinical responders and the one subject who did not respond clinically had decreased regional and whole brain HMPAO uptake. EPI-743 has modified disease progression in >90% of patients in this open-label study as assessed by clinical, quality-of-life, and non-invasive brain imaging parameters. Data obtained herein suggest that EPI-743 may represent a new drug for the treatment of inherited mitochondrial respiratory chain disorders. Prospective controlled trials will be undertaken to substantiate these initial promising observations. Furthermore, HMPAO SPECT imaging may be a valuable tool for the detection of central nervous system redox defects and for monitoring response to treatments directed at modulating abnormal redox.

1. Introduction

Inherited mitochondrial diseases are a family of disorders that share a common element in defective cellular energy metabolism [1]. While an estimated 1 in 5000 individuals are affected by mitochondrial disease caused by mitochondrial DNA (mtDNA) abnormalities, many children with signs and symptoms of mitochondrial disease lack a definitive genetic diagnosis and an increasing number of conditions that affect mitochondrial respiratory chain function have been related to nuclear DNA (nDNA) mutations, so the true prevalence of these

Abbreviations: ARE, antioxidant response element; BSO, L-buthionine-(S,R)-sulfoximine; FRDA, Friedreich ataxia; HMPAO, technetium-99m-hexamethylpropyleneamine oxime; KSS, Kearns–Sayre syndrome; LHON, Leber hereditary optic neuropathy; LS, Leigh syndrome; MELAS, Mitochondrial encephalomyopathy, lactic acidosis and stroke-like episodes; NMDAS, Newcastle Mitochondrial Disease Adult Scale; NPMDS, Newcastle Paediatric Mitochondrial Disease Scale; POLG, Polymerase gamma-1 deficiency; SPECT, single-photon emission computed tomography.

* Corresponding author at: Department of Pediatrics, Division of Medical Genetics, 300 Pasteur Drive, H-315, Stanford, CA 94305-5208, USA. Fax: +1 650 498 4555.
E-mail address: greg.enns@stanford.edu (G.M. Enns).

1096-7192 © 2011 Elsevier Inc. Open access under CC BY-NC-ND license.
doi:10.1016/j.ymgme.2011.10.009

disorders may be significantly higher [2,3]. There are no approved drug treatments for inherited mitochondrial disease [4], and these conditions are associated with substantial morbidity and mortality.

In addition to impaired ATP synthesis, inherited mitochondrial disorders manifest a variety of biochemical redox disturbances [5]. Alterations in cellular redox state have been implicated in the pathogenesis of these diseases through several mechanisms, including increased oxidative stress, depletion of cellular antioxidant defense systems, such as glutathione, and acceleration of programmed cell death [6,7]. Therefore, it is understandable that the predominant strategy employed to treat mitochondrial disease has focused on the use of antioxidants to target the oxidative stress axis of these conditions [8]. While a variety of antioxidants and cofactors have been studied, coenzyme Q_{10} (CoQ_{10}) has received the most detailed examination [4,9–13]. Results from over 50 clinical trials of CoQ_{10} suggest a marginal but real treatment effect [4]. To improve upon the bioavailability of CoQ_{10}, a truncated side-chain analog—idebenone—was developed over a decade ago and has been repurposed to treat inherited mitochondrial disease. There have been reports of idebenone improving some clinical parameters in MELAS and LHON patients [14–16]. Modest improvement in cardiac or neurological function following the use of idebenone in Friedreich ataxia patients has also been described, although recent double-blind trials have not noted statistically significant clinical effects [17,18].

Based on results obtained with CoQ_{10} and idebenone, we set out to design and test a *para*-benzoquinone analog with improved pharmacologic properties and therapeutic efficacy. Design considerations were implemented for EPI-743 to avoid the potential of mitochondrial respiratory chain inhibition or uncoupling as previously demonstrated with idebenone [19]. Our strategy centered on the synthesis of a rational series of *para*-benzoquinone analogs that systematically differed in redox potential of the quinone ring and the structure of the lipid sidechain. The result of this optimization effort is EPI-743 (Fig. 1) [20]. EPI-743 is approximately one thousand- to ten thousand-fold more potent than CoQ_{10} or idebenone in protecting cells subjected to oxidative stress in patient fibroblast assays modeling the effects of mitochondrial disease. The biological activity of EPI-743 depends upon the intrinsic properties of the *para*-benzoquinone moiety to undergo a reversible two electron cycling reaction, as is demonstrated by the inactivity of a redox-silent version (bis-pivoyl adduct) of EPI-743 in cell assay systems [20].

Because of EPI-743's favorable efficacy and safety profile, and in light of the predictable mortality associated with end-stage mitochondrial disease and absence of approved therapies, the United States Food and Drug Administration granted approval to use EPI-743 to treat patients with genetically confirmed mitochondrial respiratory chain disease who were considered to be within 90 days of end-of-life care. To augment clinical evaluation of EPI-743, we employed technetium-99m-hexamethylpropyleneamine oxime (HMPAO) single-photon emission computed tomography (SPECT) radionuclide imaging, an *in vivo* technique that has the potential to detect alterations in brain redox state [21]. While this property has not been fully appreciated or understood, the ability of HMPAO to serve as a redox sensor suggested that HMPAO SPECT has possible utility in the study of the redox imbalance that is central to mitochondrial disease pathogenesis. Herein we report the clinical data obtained in this open-label expanded access investigational new drug (IND) protocol in the first fourteen subjects treated with EPI-743 at our collaborating institutions.

2. Materials and methods

2.1. Participants

This protocol was reviewed by the Stanford University, Medical University of South Carolina, University of California, Los Angeles, CHOC Children's Hospital, and Akron Children's Hospital Institutional Review Boards. Participants were enrolled only after screening to ensure inclusion criteria, and no exclusion criteria, were met. Signed informed consent was obtained from the parents of each subject. Each of the fourteen participants (Table 1) met the two central criteria for enrollment: 1) diagnosed with a genetically defined inherited mitochondrial disease and 2) at risk for need for end-of-life (hospice) care within 90 days. Participants were asked to discontinue the use of CoQ_{10} and other antioxidant supplements for the duration of the treatment protocol. Although the clinical course of a given patient with mitochondrial disease cannot be predicted with certainly, investigators enrolled subjects who had significant morbidity secondary to their underlying condition and who were demonstrating relatively rapid progression of disease. After informed consent, cultured fibroblasts were obtained from two patients (Patients 2 and 3), for assessing response to EPI-743 *ex vivo* (Fig. 2), and performing antioxidant response element (ARE) expression analyses (Table 2).

2.2. Procedures

A baseline physical examination, standard chemistry and hematology panels, functional and quality-of-life assessment (modules I–IV, Newcastle Paediatric Mitochondrial Disease Scale [NPMDS] or Newcastle Mitochondrial Disease Adult Scale [NMDAS]) [22,23] were obtained for all patients. Serial HMPAO SPECT brain scans [21,24] were performed in 12 patients. Therapy was initiated at an EPI-743 test dose of 50 mg twice per day via mouth or gastrostomy tube for 14 days. Because no drug-related adverse clinical or

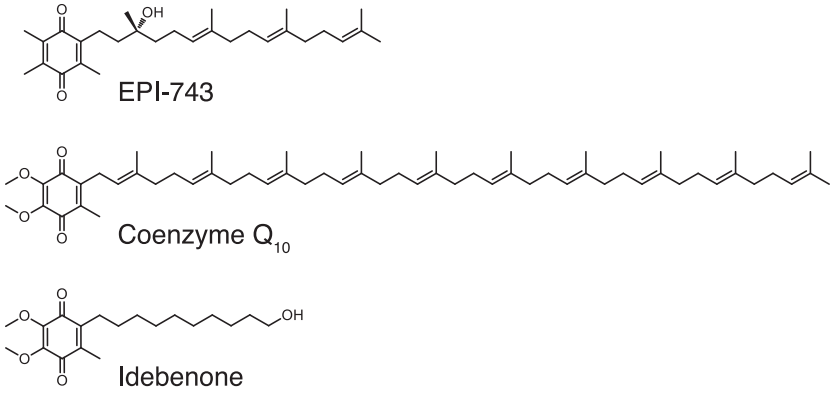

Fig. 1. Chemical structures of EPI-743, coenzyme Q_{10} and idebenone. EPI-743 is an orally bioavailable molecule that readily crosses the blood–brain barrier with a preclinical no-observable-adverse-effect level of 100 mg/kg. In addition to a truncated isoprene tail, EPI-743 possesses an important change in the quinone ring substitution pattern. In comparison to the *bis*-methoxy groups of coenzyme Q_{10} and idebenone series, EPI-743 possesses a *bis*-methyl substitution pattern that undergoes oxidation-reduction at a redox potential offset by −75 mV in comparison to coenzyme Q_{10} and idebenone [20].

laboratory events were observed, EPI-743 dose was escalated on day 15 to 100 mg, two times per day, and increased to three times per day on day 29. The protocol duration for each participant is 12 weeks. At the end of the protocol period, surviving patients were enrolled in a long-term extension that is ongoing. At the time of submission of the data reported herein, all surviving patients remain on therapy, with duration of treatment ranging from three to 14 months. Patient 2 (polymerase γ deficiency) had a 2-month trial dose reduction to 50 mg three times per day 6 months after starting EPI-743, but the EPI-743 dose has again been increased to 100 mg three times per day.

2.3. Brain HMPAO SPECT studies

HMPAO studies were obtained at the treatment hospital for each patient with the exception of Patient 1 (from UCLA), who was tested at Stanford. The Infinia™ Hawkeye 4 SPECT/CT (GE Healthcare) scanner was used for the Patients 1–3 and 5–11 (Stanford Nuclear Medicine Clinic) with the following parameters; start at 0°, 180° rotation/detector, 64 steps, 2.8125° per step, 22 seconds per step, overall ARC 360°, (scan time = 23 minutes) 128 × 128, multipurpose collimator (Skylight) in zoom mode; ROR—min. Patient 14 was scanned (Akron Children's Hospital) with a Philips Brightview Dual Head SPECT/CT Scanner using the same parameters as above, with the exception that 128 steps instead of 64 steps were acquired. Patient 4 was scanned (Medical University of South Carolina) with an earlier model of the GE Hawkeye, dual detector, SPECT/CT Scanner (Millenium VG System) with 360 degrees of data sampling (180 degree per detector), a 128 × 128 matrix using a "step and shoot" protocol at 6 degree stops for 30 seconds each. Age-based reduction of an adult 925 MBq dose of HMPAO [according to Webster's Rule = ((AGE (IN YEARS) + 1 YEAR) × STANDARD ADULT DOSE) /AGE + 7 was used to adjust dosing of tracer at Stanford (the single patient from UCLA was imaged at Stanford) and Akron. Weight-based dosing utilizing Gilday's Chart for reduction in children of a 1110 MBq adult dose of HMPAO was used at the Medical University of South Carolina. All cameras at each institution were peaked at 140 keV with 10% window. All scans started 30 to 40 minutes after injection of tracer with the patients at rest in a darkened room. After reconstruction, volumetric image analyses were performed with the statistical parametric mapping program SPM 94 [25]. This program standardizes brain position and voxel content based on the brain atlas and methodology of Talairach and Tournoux [26]. All volumetric data sets were acquired, processed and analyzed without magnification to avoid potential errors in obtaining accurate absolute counts from each region of interest. Summed counts were obtained from region of interest analyses of the whole cerebrum and the right and left cerebral hemispheres. The total counts value for each region was then divided by the number of elements (voxels) generated by the mapping program and the amount of injected activity expressed in millicuries (mCi) to obtain average normalized HMPAO uptake (i.e. = counts/element/mCi) for the cerebrum and each cerebellar hemisphere. Using the elements generated by the mapping program instead of actual voxel size also effectively normalized the brain volume of each subject to allow for easier comparison of regional uptake of HMPAO between different sized subjects.

The average uptake of the cerebrum (counts/element/mCi) was then substituted for average cerebral uptake generated by the mapping program (which is expressed by the software as the % of maximal brain uptake/element). This permitted the calculation of the average normalized counts per element for all cerebral (i.e. supratentorial) regions and Brodmann cortical areas instead of the dimensionless parameter, average % of max brain uptake/element, tabulated by SPM 94.

Z-scores generated by the mapping program were also tabulated. The normal population used by the program consistent of 64 patients ranging from 16 to 45 years (the youngest set of normal standards available at this time).

2.4. Cultured fibroblast response to oxidative stress and EPI-743 supplementation

2.4.1. EPI-743 rescue from oxidative stress

Age- and sex-matched wild-type control fibroblasts (GM00038) were obtained from Coriell. Fibroblast cell lines from the controls and Patients 2 and 3 were assayed prior to passage 10. Assays were conducted in glucose-free DMEM supplemented with 1 mM pyruvate, 10% FBS and PS (Gibco). Cells were incubated with the glutathione synthesis inhibitor L-buthionine-(S,R)-sulfoximine (BSO, 50 μM) over 88 h.

2.4.2. ARE expression analysis

Primary fibroblasts from Patient 2 were treated with DMSO vehicle, 1uM EPI-743 or redox silent EPI-743 (RS-EPI-743) overnight. The next day, glutathione was depleted using BSO, and RNA harvested prior to initiation of cellular death (24 h post stress). After conversion to cDNA with Transcriptor First Strand Kit, the Roche LC480 UPL system was used to amplify and calculate relative quantities of gene expression (experiment was performed in quadruplicate and all results are expressed as a ratio of test condition to vehicle treated cells).

2.5. Pharmacokinetics

The analysis of EPI-743 was performed using an Agilent 1100 HPLC connected to a Sciex API 5000 triple quadrapole LC-MS/MS with a Turbo V Ion Spray Source. The HPLC chromatography used a Zorbax eclipse plus phenyl-hexyl 1.8 μm, 2.1 × 50 mm analytical column, with an aqueous phase of acetic acid, 1 M ammonium acetate, water (2/2/96 - v/v/v) and an organic phase of acetonitrile. This bioanalytical method was determined to be accurate and precise in the validated calibration range from 1.00 to 1000 ng/mL. Samples with a concentration higher than the upper limit of quantification (ULOQ) were accurately quantified by diluting the samples up to a 20-fold dilution with blank matrix, to achieve a concentration within the range of the calibration curve. All processed plasma samples of EPI-743 were exposed to air to fully oxidize EPI-743 to its quinone state before LC/MS/MS quantification. Deuterated EPI-743 (d_4-EPI-743) was used as an internal standard. All EPI-743 analyses were conducted in compliance with FDA's Good Laboratory Practices (21 CRF Part 58) using a validated method developed in accordance to the FDA Guidance for Industry for Bioanalytical Method Validation. All samples were analyzed by MPI Research, Inc. (State College, PA, USA).

2.6. Statistical analyses

The non-parametric Wilcoxon paired rank sum test was used to compare baseline and 13-week NPMDS scores and for HMPAO SPECT analyses. *P*-values < 0.05 were considered significant. Statistical comparisons for fibroblast data were made using a two-tailed Student's *t*-test of significance.

3. Results

3.1. Newcastle Paediatric Mitochondrial Disease Scale (NPMDS) scores

Over the 3-month course of this treatment protocol, the NMPDS total scores (Sections I through IV combined) and quality-of-life scores (Section IV) showed significant overall improvement from baseline in all surviving pediatric participants ($P = 0.004$). One patient (Patient 5) showed a mild worsening in the NPMDS at 3 months with no change in the quality-of-life score at this time point. (However, Section IV was repeated again 9 months after starting the treatment in Patient

Table 1
Patient clinical features, laboratory and imaging findings. The Newcastle Paediatric Mitochondrial Disease Scale (NPMDS) was used to both stage (baseline) and gauge clinical response (after 3 months of therapy) in pediatric subjects and the Newcastle Mitochondrial Disease Adult Scale (NMDAS) was used in the single adult subject. The NPMDS and NMDAS are divided into four categories and scores are shown for each sub-section. Section I (Function) relates to current function during the preceding 4-week period; Section II (System Specific Involvement) documents severity and range of clinical problems across multiple organ systems over the preceding 12-month period; Section III (Current Clinical Assessment) describes the clinical status at the time of the evaluation; and Section IV (Quality of Life) is a questionnaire that relates to the past 4 weeks. NB: Lower scores indicate less severe disease burden for NPMDS Sections I to IV and NMDAS Sections I to III. A higher score indicates better quality-of-life for NMDAS Section IV (Short Form-12v2) (Patient 7).

Patient	Age, weight, gender	Clinical diagnosis	Genetic diagnosis	EPI-743 dosing duration[b]	EPI-743 Plasma C_{max}[c]	Brain Imaging[d]	Clinical response	NPMDS scores		
								Section	Baseline	After therapy
1	17 years 52 kg Female	FRDA	Compound heterozygous *FXN* mutations (963GAA repeat expansion, novel point mutation [p.W155R])	444 days	82 ng/mL	MRI (16 years, 9 months): Mild enlargement of third and fourth ventricles and prepontine and interpeduncular cisterns MRS (16 years, 9 months): Small cerebellar lactate peak	Improved strength, exercise tolerance, speech fluency, sleep, increased social interaction, regaining of partial eye sight after 7 months with the ability to read large block letters following several years of complete cortical blindness	I II III IV Total	15 5 20 10.5 50.5	15 5 20 7.4 47.4
2	13 years 35 kg Female	POLG	Homozygous *POLG1* mutations (c.9iiT>G [p.L340R])	419 days	257 ng/mL	MRI (13 years, 6 months): Normal MRS (13 years, 6 months): Normal	Improved exercise tolerance, strength and speech fluency over 3 months, followed by increasing weakness, especially proximally, but retention of cognitive abilities	I II III IV Total	7 3 18 9.8 37.8	4 2 18 7.3 31.3
3	11 years 25 kg Male	KSS	4,977 kb "common" mtDNA deletion	355 days	517 ng/mL	MRI (8 years, 4 months): Signal intensity abnormalities in cerebral white matter, globus pallidi, thalami, midbrain, pontine tegmentum, cerebellar hemispheres MRS (8 years, 4 months): Central gray matter lactate peaks	Improved strength, exercise tolerance, speech fluency, sleep, increased social interaction, decreased insulin requirements, progression of pigmentary retinopathy	I II III IV Total	16 10 18 19.6 63.6	15 10 17 12.4 54.4
4	11 years 32 kg Female	MELAS	3243A>G mtDNA	306 days	117 ng/mL	MRI (11 years, 3 months): Areas of abnormal cortical signal within the insular lobes bilaterally and left parietal lobe, T2 signal abnormalities within the right parietal and temporal lobes with associated parenchymal atrophy	Improved seizure control, strength, exercise tolerance, speech fluency, sleep, and increased social interaction	I II III IV Total	17 11 15 25.4 68.4	16 11 17 20.4 64.4
5	8 years 22 kg Male	Dystonia[a]	3243A>G mtDNA	264 days	124 ng/mL	MRI (8 years, 6 months): Prominent perivascular space in the right anterior corona radiata MRS (8 years, 6 months): Normal MRI (8 years, 8 months): High T2/ FLAIR signal focus in right caudate head, acute ischemic lesion in right cerebellar hemisphere MRI (8 years, 10 months): Normal	Improved choreoathetosis, sleep, increased social interaction, starting to use sign language	I II III IV Total	17 9 18 18.8 62.8	17 12 18 18.8 65.8
6	5 years 7 kg Male	LS	Heterozygous *SURF1* mutations (c.240+1G>T [p.Q80fsX90]; c.516-2AA>G [p.V172fsX183])	223 days	235 ng/mL	MRI (11 months): Abnormal T2 hyperintensity in bilateral basal ganglia	Improved strength, energy, social interaction	I II III IV Total	15 4 16 21.3 56.3	14 6 16 7.1 43.1
7	27 years 63 kg Male	MELAS	3243A>G mtDNA	222 days	66 ng/mL	MRI (22 years): Bilateral cortical infarction, slightly prominent ventricles MRI (22 years, 7 months): Moderately severe cerebral and cerebellar atrophy, multiple diffuse, symmetric areas of cortical encephalo-malacia, acute ischemia left insular area	Improved speech fluency, increased social interaction	I II III Total SF-12v2[e]	10 14 6 30 72.7	9 13 6 28 85.2

Table 1 (*continued*)

Patient	Age, weight, gender	Clinical diagnosis	Genetic diagnosis	EPI-743 dosing duration[b]	EPI-743 Plasma C_{max}[c]	Brain Imaging[d]	Clinical response	NPMDS scores		
								Section	Baseline	After therapy
						MRI (24 years, 7 months): Extensive areas of abnormal signal intensity and volume loss involving the cerebral hemispheres bilaterally, diffuse cerebral and cerebellar atrophy				
8	4 years 12 kg Female	Pearson syndrome	4,977 kb "common" mtDNA deletion	213 days	262 ng/mL	MRI (4 years, 1 month): Normal MRS (4 years, 1 month): Normal	Improved sleep pattern and energy, normalization of hematocrit and platelet counts initially; reverted to baseline following 3 hospitalizations for pancreatitis, urinary tract infections and *Clostridium difficile* enteritis, developed mild hypothyroidism, continues to make gains in energy and interaction following most recent hospitalization	I II III IV Total	4 11 4 15.8 34.8	1 11 2 14.2 28.2
9	2 years 10.2 kg Male	Leigh syndrome	Heterozygous *SURF1* mutations (c.312_321del10insAT [p.L105X]; c.845_846delCT [p.S282CfsX9])	207 days	634 ng/mL	MRI (28 months): Signal abnormalities in the basal ganglia and brainstem MRS (28 months): Lactate peaks	Stabilization and improved energy, strength and social interaction, gaining developmental milestones; died suddenly after developing respiratory symptoms considered to be caused by brainstem disease	I II III IV Total	13 3 12 17.1 45.1	13 4 13 10.4 40.4
10	6 years 17.2 kg Male	Leigh syndrome	10158T > C mtDNA (65% mutant load in whole blood)	199 days	100 ng/mL	MRI (22 months): Symmetric increased T2 signal in basal ganglia, inferomedial thalamus, periaqueductal gray matter and substantia nigra MRI (3 years, 5 months): Increased T2 signal involving bilateral putamen, caudate heads and globus pallidus MRI (6 years, 9 months): Diffuse right cerebral edema, focal area of right frontal ischemia, areas of low density within the basal ganglia, areas of hyperdensity within the left caudate nucleus and internal capsule	Initial stabilization of disease and improved energy, strength, speech fluency, and social interaction; loss of gains and worsening seizures following hospitalization for stroke-like episode, continues to improve in speech fluency and energy following hospitalization	I II III IV Total	11 1 16 11.7 39.7	8 3 14 10.8 35.8
11	4 years 12.2 kg Female	Alpers syndrome	*POLG1* mutations (heterozygous for c.2740A > C [p.T914P] and c.229C > G [p.Q77E]; homozygous for c.1399G > C [p.A467T])	143 days	115 ng/mL	MRI (3 years , 8 months): Normal	Improved strength, energy, sleep, social interaction and diminished intensity of myoclonus	I II III IV Total	14 8 18 17.1 57.1	14 8 18 12.9 52.9
12	7 years Female	Alpers syndrome	Heterozygous *POLG1* mutations (c.2243G > C [p.W748S]; c.3428A > G)	9 days	197 ng/mL	MRI (7 years, 7 months): T2 and Flair hyperintensity in bilateral thalami MRS (7 years, 7 months): Normal	No effect; died of pneumonia 9 days after starting EPI-743	I II III IV Total	17 12 15 19.6 63.6	NA NA NA NA NA
13	2 years 10.6 kg Female	Leigh syndrome	Heterozygous *SURF1* mutations (c.311-12insAT311_321 [p.P104fsX1]; c.845-846delCT [p.S282fsX9])	115 days	441 ng/mL	MRI (18 months): Symmetric T2 signal abnormalities in the corticospinal tracts, periaqueductal gray matter, and medulla, diffuse abnormal enhancement in the excitatory nerve roots throughout the cervical, thoracic, and lumbar spine MRI (22 months): Advancement of T2 signal	Improved nystagmus, pulmonary function, swallowing, and sleep, increased interaction and acquisition of milestones over 4 months, followed by loss of motor skills after an episode of tracheitis	I II III IV Total	13 8 13 10.4 44.4	13 7 11 4.6 35.6

(*continued on next page*)

Table 1 (*continued*)

Patient	Age, weight, gender	Clinical diagnosis	Genetic diagnosis	EPI-743 dosing duration[b]	EPI-743 Plasma C_{max}[c]	Brain Imaging[d]	Clinical response	NPMDS scores		
								Section	Baseline	After therapy
						abnormalities, new areas of abnormal T2 prolongation in left basal ganglia MRS (22 months): Left basal ganglia lactate peaks				
14	2 years 19 kg Male	Alpers syndrome	*POLG1* mutations (c.1388G > C [p.A467T]; c.32G > A [p.G11D] + c.2554C > T [p.R852C])	98 days	20 ng/mL	MRI (11 months): Normal	Increased interaction, vocalization, and movement, normalization of opticokinetic response, decreased seizure frequency, persistence of tremor and myoclonus	I II III IV Total	18 7 16 10.8 51.8	16 6 13 9.6 44.6

Abbreviations—FRDA = Friedreich ataxia; KSS = Kearns–Sayre syndrome; LS = Leigh syndrome; MELAS = Mitochondrial encephalomyopathy, lactic acidosis and stroke-like episodes; NPMDS = Newcastle Paediatric Mitochondrial Disease Scale; POLG = Polymerase gamma-1 deficiency.

[a] Patient 5 does not have a classical MELAS phenotype, but rather neurological disease characterized by severe dystonia and choreoathetosis.

[b] Total days of EPI-743 treatment (until August 15, 2011).

[c] Peak plasma concentration (C_{max}) obtained from a single 50 mg dose, and sampled between 1 and 3 h.

[d] Pre-treatment brain imaging results using standard techniques are shown.

[e] The adult subject (Patient 7) was assessed using the Newcastle Mitochondrial Disease Adult Scale (NMDAS); the quality-of-life instrument used for the NMDAS and this subject was the SF-12v2.

5 and had improved to 9.2). Although patients demonstrated clinical improvements following treatment with EPI-743, including increased strength, requiring less support to ambulate, better balance and improved speech fluidity, when NPMDS Sections I through III were combined (i.e. excluding the quality-of-life measurement) no significant change was observed. The single adult subject also had improvement in overall NMDAS score and quality-of-life as determined by Short Form-12v2 assessment (Table 1).

3.2. Clinical evaluations

Twelve of fourteen treated patients have survived to date and demonstrate clinically significant signs and symptoms of improvement independent of age (2 to 27 years) or genetic defect origin (mtDNA versus nDNA) (Table 1). Objective improvements were noted in cardiac function, glucose tolerance, muscle strength, exercise tolerance, social interaction, speech fluidity, and sleep duration and quality. Patient 5 showed only brief clinical improvement during the first week of EPI-743 therapy, but then worsened throughout the duration of the 3-month protocol. However, pharmacokinetic data obtained at the conclusion of the 3-month protocol showed that he had absorbed EPI-743 poorly after the first week of treatment. The delivery of EPI-743 was then altered by first mixing with an elemental formula, which resulted in increased absorption similar to other subjects (see Section 3.6 Pharmacokinetics below) and rapid clinical improvement. Conversely, Patient 2 showed steady improvement during the course of the treatment protocol, but has since manifested increased weakness, although cognitive skills have been preserved. Subjectively, all subjects, their care providers, or both noted an increase in energy and less physical and mental fatigue. Further details about each subject are provided in the online Supplemental Data.

3.3. Brain HMPAO SPECT imaging (EPI-743 3-month treatment protocol)

HMPAO was used to assess changes in brain redox state serially during treatment with EPI-743 because of its sensitivity to intracellular redox status and reduced glutathione concentration [21,24,27,28]. SPECT imaging at baseline revealed substantially lower HMPAO uptake as compared with aged-matched standardized population volumetric-anatomic computerized image data sets as shown in Fig. 3. All patients had substantially decreased brain HMPAO uptake at baseline either within the cerebrum or cerebellum at study entry, with most patients demonstrating decreased uptake in multiple brain anatomic sites (Fig. 3). Whole brain HMPAO uptake increased significantly from baseline when compared to SPECT scan results at 3 months ($n = 12$, $P = 0.0186$). The increase in HMPAO was greater in the deep gray matter when compared to brain cortex uptake ($P = 0.0025$), but no significant difference in uptake was observed when deep gray matter was compared to the cerebellum (Fig. 4). Over the course of the 3-month protocol, clinical improvement correlated with an increase in HMPAO uptake as determined by brain SPECT in all study patients who had this assessment performed ($n = 12$) and who had an improved clinical course. Patient 8 (Pearson syndrome) was the only subject who had a fall in HMPAO uptake in all areas of the brain during the initial 3-month protocol, but her clinical status at the time of the 3-month scan had not improved compared to baseline (see Supplemental Data).

3.4. Brain HMPAO SPECT imaging (EPI-743 extension protocol)

Five patients underwent HMPAO SPECT brain scans during an extension phase of the protocol (past the initial 3-month duration). At 12 months, Patient 1 (Friedreich ataxia) showed continued gradual improvement in overall HMPAO uptake on SPECT imaging, with whole brain HMPAO uptake increasing from 39% to 56% (Fig. 5). During this period, Patient 1 demonstrated regaining of partial eyesight after several years of complete cortical blindness and continued to make steady improvements in speech fluidity and motor skills.

Patient 2 (polymerase γ deficiency) was one of three subjects who did not show increase in all brain areas with longitudinal follow-up. She showed an increase in whole brain HMPAO uptake of 22% over the initial 3-month protocol period, during which time she was noted to have clear clinical improvement, including increased strength and mobility. Increasing ataxia and weakness was noted about 4 months after initiating therapy, and brain HMPAO SPECT imaging was repeated at 5 months; compared to baseline, a substantial decrease in HMPAO uptake was noted in the putamen and thalamus. Despite the general falloff of tracer uptake in multiple brain areas, whole brain uptake was still increased by 10% compared to baseline. The relatively stable cerebral cortical uptake of HMPAO observed at 5 months correlated with the preservation of cognitive function despite increasing ataxia and weakness. At 8 months, the dose of EPI-

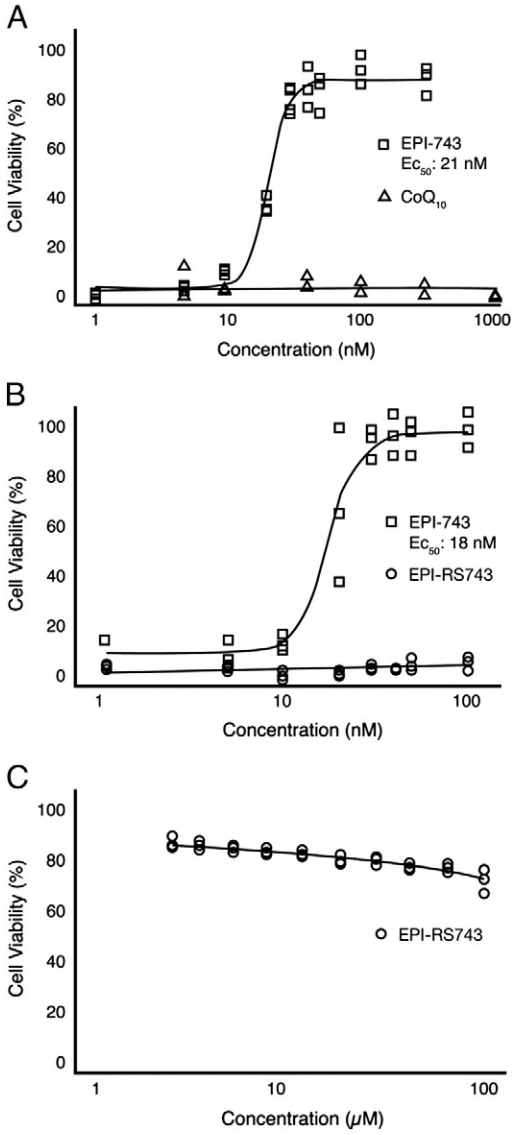

Fig. 2. Cultured fibroblast response to oxidative stress and EPI-743 rescue. (A) Skin fibroblasts isolated from Patient 2 (polymerase γ deficiency) were treated with the glutathione synthesis inhibitor L-buthionine-(S,R)-sulfoximine before adding either EPI-743 or coenzyme Q_{10} to the culture media. The addition of EPI-743 to culture media protected cells from death with an EC_{50} (half maximal effective concentration) of 21 nM, while coenzyme Q_{10} did not have an effect up to a concentration of 1000 nM. (B) Fibroblasts from Patient 3 (Kearns–Sayre syndrome) were treated as above, with similar results; EPI-743 protected cells from death with an EC_{50} of 18 nM, while coenzyme Q_{10} did not have an effect up to a concentration of 100 nM. (C) The GI_{50} (50% growth-inhibitory concentration) for a redox-silent form of EPI-743 (RS-EPI-743) was greater than 100 μM, so the lack of cellular rescue of this compound in (B) was not secondary to compound toxicity.

743 was decreased to 50 mg three times daily during a period of further disease progression, because she initially had clinical improvement on the lower dose, as well as a theoretical concern that the retrograde signal for mitochondrial proliferation may have been altered or dampened by EPI-743; animal models have provided data that suggest that redox imbalance may play a relatively small role in disease pathogenesis in polymerase γ deficiency [29]. This dose reduction, however, was followed by a more rapid progression of symptoms characterized by increasing weakness, inability to walk, and declining respiratory function, so EPI-743 administration was increased again to 100 mg three times daily. The most recent HMPAO SPECT scan in Patient 2 was performed at 10 months following initiation of EPI-743 treatment (2 months after increasing the EPI-743 dose) and showed remarkable increases of HMPAO uptake in all brain areas, with the whole brain uptake increasing to 61% (Fig. 5). This increased uptake occurred during a period of stabilization of her disease status and improvement in respiratory function (see Supplemental Data).

Patient 3 (Kearns–Sayre syndrome) appeared to have stable whole brain HMPAO uptake at 10 months following institution of EPI-743 treatment compared to the 3-month time point, although there was decreased uptake especially in the caudate and cerebellum compared to the baseline scan. He had made relatively rapid improvements during the first 3 months of the treatment protocol and these gains were maintained at the 10-month time point, although his parents reported at that time that progress was being made at a slower pace. Despite motor and cognitive gains, however, his pigmentary retinopathy has continued to worsen despite EPI-743 treatment.

Patient 5 (choreoathetosis, MELAS 3243A>G) had virtually unchanged HMPAO uptake in the caudate nucleus and a relatively mild overall increase in whole brain HMPAO uptake (8%) at the 3-month SPECT scan, performed during the last few days of a nearly 3 week pentobarbital induced coma for control of choreoathetoid movements. A further SPECT scan performed at 4 months, taken while Subject 5 had been started on phenobarbital, showed surprisingly low levels of HMPAO uptake, given the marked clinical improvement demonstrated following improved absorption of EPI-743. This discordance between the changes in clinical status and brain HMPAO uptake in Patient 5 may have been related to enhanced biliary excretion of the radiotracer secondary to chronic high-dose barbiturate and phenobarbital use [30–32].

The clinical status of Patient 7 (MELAS 3243A>G) appeared to be similar 5 months after the initiation of EPI-743 therapy compared to the 3-month evaluation. Although whole brain HMPAO uptake also appeared similar, he demonstrated a clear decrease in HMPAO uptake in the putamen, thalamus, and cerebellum.

3.5. Pharmacokinetics

EPI-743 peak plasma (C_{max}) levels were obtained in all subjects after a single 50 mg dose via mouth or gastrostomy tube (Table 1). The C_{max} occurred between 1 and 3 h after dosing and ranged from 20 ng/mL to 634 ng/mL (mean 226.2 ng/mL SD ± 249.9 ng/mL). Subject 5 demonstrated good EPI-743 absorption during week 1, but had poor absorption throughout the remaining duration of the 12-week protocol (mean C_{max} = 28 ng/mL ± SD 23 ng/mL, n = 4, weeks 2 to 15). Absorption improved following mixing of EPI-743 with an elemental formula before delivery (C_{max} = 326 ng/mL). Subject 8 also demonstrated good EPI-743 absorption during week 1 (C_{max} = 1080 ng/mL), with poor absorption following worsening gastrointestinal symptoms (C_{max} = 18.3 ng/mL).

3.6. Adverse events

No participants experienced a drug-related serious adverse event (SAE). However, several subjects experienced SAEs related to their underlying disease (e.g. choreoathetosis, gastrointestinal dysmotility, seizures, persistent myoclonus, stroke-like-episode) or SAEs related to infections (e.g. pneumonia, gastroenteritis, urinary tract infection, central line infections) that required hospitalization but were judged to be unrelated to the study drug. Patient 12 developed pneumonia soon after starting EPI-743 and died after support was withdrawn. Patient 9 died suddenly after developing respiratory failure related to brainstem dysfunction 8 months after starting treatment. Patient 8 had an episode of elevated liver transaminases (4 to 8 times upper limit of normal [ULN]) lasting several weeks after hospitalization and treatment for a urinary tract infection, with resolution following treatment with *N*-acetylcysteine. Patient 14 was hospitalized briefly on two occasions, once for possible pneumonia and once for pancreatitis.

Table 2
Effects of EPI-743 on ARE family gene expression during cellular stress.

Gene symbol	Gene name	E.C. number	Function	Stress	Stress + EPI-743 (±SD)	Stress + RS-743 (±SD)	EPI-743 (±SD)
HMOX1	Heme oxygenase 1	1.14.99.3	Cleaves heme to biliverdin	13.29 ± 2.11	3.31 ± 0.28	12.30 ± 0.96	0.48 ± 0.047
AKR1C1	Aldo-keto reductase	1.3.1.20	NAD(P)H-dependent conversion of aldehydes and ketones to alcohols	7.23 ± 1.52	2.86 ± 0.2	7.37 ± 0.65	1.05 ± 0.12
TRXR1	Thioredoxin reductase 1	1.8.1.9	Reduces thioredoxins	3.87 ± 0.79	2.39 ± 0.21	3.16 ± 0.38	1.09 ± 0.13
NQO1	NAD(P)H dehydrogenase, Quinone reductase	1.6.99.2	2 electron reduction of quinones	2.66 ± 0.39	2.06 ± 0.17	2.45 ± 0.23	0.98 ± 0.08
SRXN1	Sulfiredoxin	1.8.98.2	Reduces sulfinic acid to thiol in an ATP-dependent manner	4.66 ± 0.77	2.82 ± 0.43	3.98 ± 0.49	1.01 ± 0.11
GCLM	Glutamate-cysteine ligase	6.3.2.2	Rate-limiting enzyme of glutathione synthesis—regulatory unit	4.67 ± 0.66	2.56 ± 0.22	4.40 ± 0.46	1.04 ± 0.09
GCLC	Glutamate-cysteine ligase	6.3.2.212	Rate-limiting enzyme of glutathione synthesis—regulatory unit, inhibited by buthionine-(S,R)-sulfoximine	3.81 ± 0.55	1.79 ± 0.18	3.34 ± 0.27	1.08 ± 0.11
GSR	Glutathione reductase	3.4.11.7	Reduces GSSG to GSH	2.57 ± 0.37	1.68 ± 0.14	2.34 ± 0.21	1.08 ± 0.17
GSTO1	Glutathione *S*-transferase omega 1	2.5.1.18	Dehydroascorbate reductase activity; May function in the glutathione–ascorbate cycle	1.80 ± 0.35	0.92 ± 0.13	1.47 ± 0.19	0.67 ± 0.10

Several non-serious, but possibly drug-related, events were also reported. Patients 2 and 4 developed transient elevations of creatine kinase that were not associated with clinical symptoms. Patient 5 developed transiently elevated creatine kinase likely related to severe choreoathetosis and transiently elevated transaminases during a period of worsening gastrointestinal symptoms. Patient 3 experienced mild, self-limited loose stools for a few days after increasing to maximal dose. Patient 7 described developing insomnia during the first several weeks of therapy, but this resolved without specific treatment. Patient 8 also developed intermittent insomnia during the first few months of therapy, but her sleep pattern has now improved. Patient 11 showed mild elevation of liver transaminases (2 to 4 times ULN), but this was also considered more likely related to her underlying diagnosis of Alpers syndrome. A more complete description of adverse events is given in the Supplemental Data clinical narratives.

3.7. Fibroblast studies

3.7.1. EPI-743 rescues cell lines from oxidative damage

Results from Patient 2 and Patient 3 fibroblast assays are shown in Fig. 2a and b, respectively. While wild-type cells can tolerate L-buthionine-(S,R)-sulfoximine (BSO) exposure, mitochondrial disease fibroblasts die within 88 h. To assess the response of dysfunctional mitochondria to therapy, EPI-743 was added to cell cultures 12 h

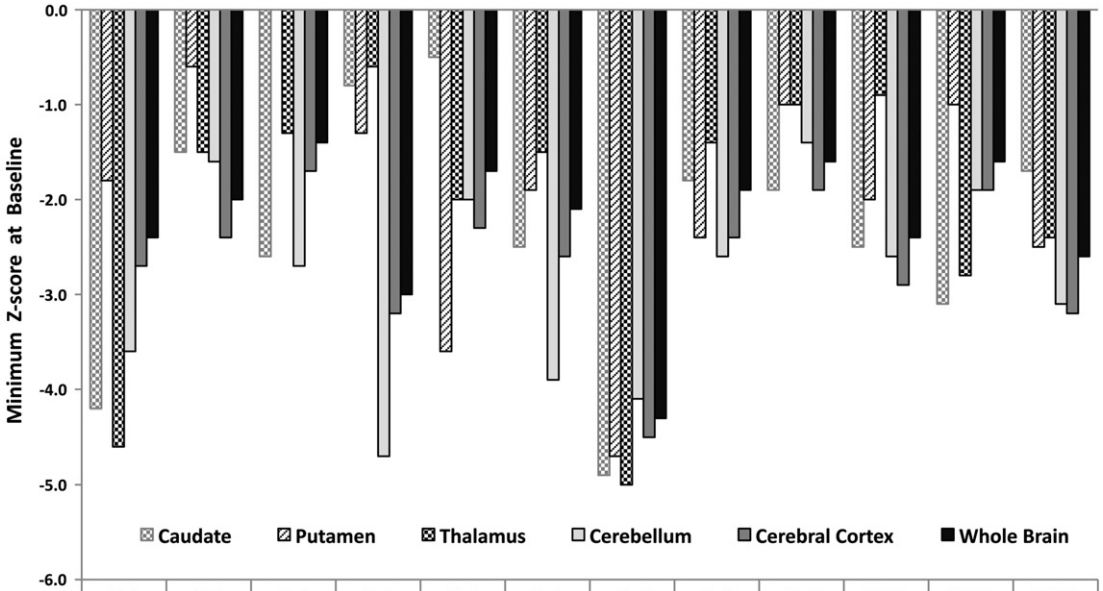

	Pt-1	Pt-2	Pt-3	Pt-4	Pt-5	Pt-6	Pt-7	Pt-8	Pt-9	Pt-10	Pt-11	Pt-14
Caudate	-4.2	-1.5	-2.6	-0.8	-0.5	-2.5	-4.9	-1.8	-1.9	-2.5	-3.1	-1.7
Putamen	-1.8	-0.6	0.9	-1.3	-3.6	-1.9	-4.7	-2.4	-1	-2	-1	-2.5
Thalamus	-4.6	-1.5	-1.3	-0.6	-2	-1.5	-5	-1.4	-1	-0.9	-2.8	-2.4
Cerebellum	-3.6	-1.6	-2.7	-4.7	-2	-3.9	-4.1	-2.6	-1.4	-2.6	-1.9	-3.1
Cerebral Cortex	-2.7	-2.4	-1.7	-3.2	-2.3	-2.6	-4.5	-2.4	-1.9	-2.9	-1.9	-3.2
Whole Brain	-2.4	-2	-1.4	-3	-1.7	-2.1	-4.3	-1.9	-1.6	-2.4	-1.6	-2.6

(a)

Fig. 3. Baseline brain HMPAO uptake. HMPAO is lipophilic in its reduced state and readily crosses the blood–brain barrier. It is subsequently trapped in neurons and astrocytes with normal redox potential after rapid conversion to a hydrophilic molecule by normal intracellular metabolism. However, when there is a redox shift towards oxidation, HMPAO changes to its hydrophilic state and cannot enter or be retained by cells and tissues affected by mitochondrial disease [21]. The degree of wash out of HMPAO (rapid loss of initial activity) in the brain or other organs, therefore, increases depending on the degree of oxidative stress. At baseline, all patients showed a decrease in brain HMPAO uptake of at least −2 *Z*-scores in one or more brain areas compared to normal controls. [a]Further segmentation of the cerebral cortex revealed *Z*-scores of −2.0 to −2.1 in the frontal lobes of Patient 9.

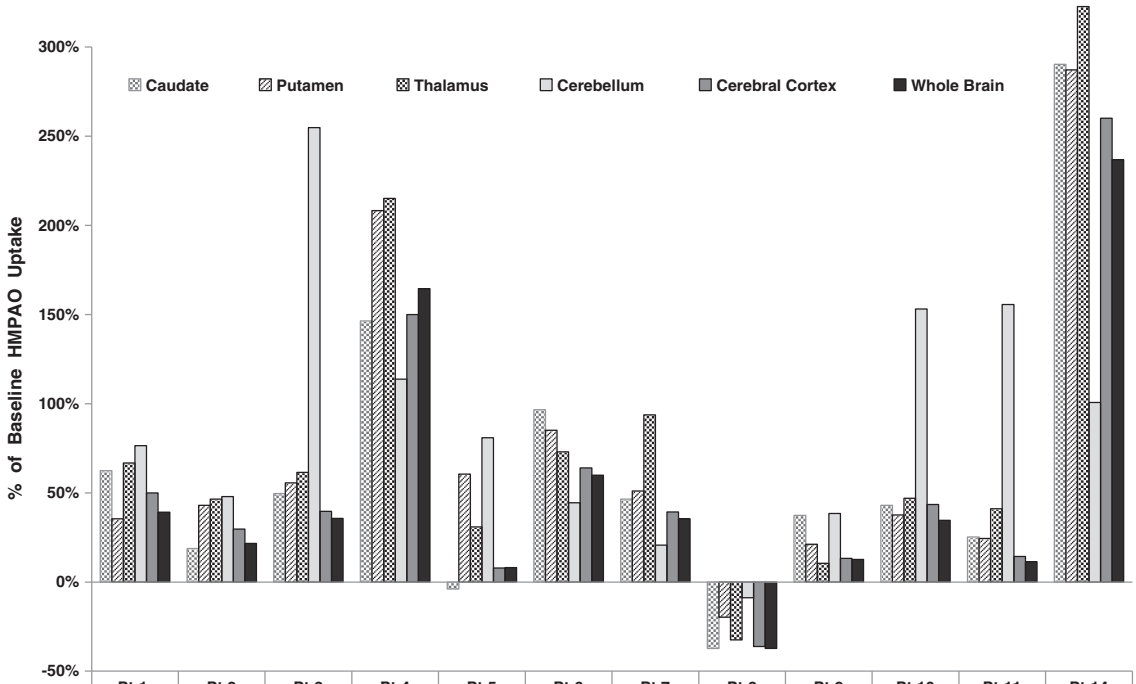

	Pt-1	Pt-2	Pt-3	Pt-4	Pt-5	Pt-6	Pt-7	Pt-8	Pt-9	Pt-10	Pt-11	Pt-14
Caudate	62%	19%	50%	146%	-4%	97%	47%	-37%	37%	43%	25%	290%
Putamen	36%	43%	56%	208%	61%	85%	51%	-20%	21%	38%	24%	287%
Thalamus	67%	46%	61%	215%	31%	73%	94%	-32%	10%	47%	41%	323%
Cerebellum	76%	48%	255%	114%	81%	44%	21%	-9%	38%	153%	156%	101%
Cerebral Cortex	50%	30%	40%	150%	8%	64%	39%	-36%	13%	43%	14%	260%
Whole Brain	39%	22%	36%	165%	8%	60%	35%	-37%	13%	35%	11%	237%

Fig. 4. Percentage change of brain HMPAO uptake compared to baseline. When patients were analyzed as a group, whole brain HMPAO uptake increased following EPI-743 treatment with a mean of 52.0% ± SD 75.1. HMPAO uptake increased in specific brain regions as follows: caudate 64.6% ± SD 84.7; putamen 74.2% ± SD 89.2; thalamus 81.3% ± SD 96.1; cerebellum 89.8% ± SD 72.7; cerebral cortex 56.3% ± SD 80.2.

before a BSO insult. Drug efficacy was expressed as % maximal cell survival at 88 h, compared to vehicle control wells. EPI-743 protected cells from death with an EC_{50} (half maximal effective concentration) of ~20 nM (Figs. 2a and b). However, a redox silent analogue compound (RS-EPI-743) assayed alongside EPI-743 did not have any effect on cell viability. RS-EPI-743 was prepared by the hydride reduction of (*R*)-α-tocotrienol quinone to the dihydroquinone, with subsequent acylation to form a bis-pivaloyl ester [20]. The GI_{50} (50% growth-inhibitory concentration) for RS-EPI-743 was found to be greater than 100 μM, so the lack of observed activity of this compound was not secondary to compound toxicity (Fig. 2c).

3.7.2. Pre-treatment with EPI-743 decreases cellular stress response

The most significant changes in fibroblasts obtained from Patient 2 were observed for antioxidant response element (ARE) genes under the direct control of nuclear factor-erythroid 2 p45-related factor (Nrf2), a transcription factor that regulates expression of a number of antioxidant enzymes. Oxidative stress greatly increased the expression of *HMOX1* (50x) and other members of ARE genes to various degrees. Pre-treatment with EPI-743 blocked the ARE response, resulting in decrease of *HMOX1* to 8 times of basal levels, and significantly reducing the expression of other ARE genes (Table 2). These data suggest that pretreatment with EPI-743 allows the cell to cope with the oxidative stress that otherwise would have induced a major cellular stress response. Importantly, pre-treatment with the RS-EPI-743 did not result in similar suppression of stress-induced ARE gene upregulation as observed with EPI-743, further supporting the critical importance of redox cycling of EPI-743 for its activity. EPI-743 or RS-EPI-743 treatment alone, in the absence of induced oxidative stress, did not affect expression in any of the genes tested (Table 2).

4. Discussion

The development of drug therapies for rare and heterogeneous pediatric diseases is fraught with challenges [33]. Inherited mitochondrial diseases are particularly difficult therapeutic targets, given their complex genetics, varied clinical presentations, lack of predictive laboratory models, and absence of clinical tools to judge therapeutic efficacy [4,34]. These challenges have resulted in significant technical and clinical impediments to drug discovery and development initiatives [35,36].

EPI-743 was developed through a chemocentric approach focusing on making systematic changes to the redox head and lipid tail of CoQ_{10}. Pre-clinical data obtained prior to commencement of human studies suggested that EPI-743 was safe, orally absorbed, and penetrated the central nervous system [20]. We treated thirteen children and one adult with severe manifestations of mitochondrial disease where the risk of untoward drug effect was outweighed by the poor prognosis. Participants were selected based on two criteria: i) genetically confirmed mitochondrial disease; and ii) possibility of end-of-life care starting within 90 days. Subjects were consecutively enrolled with genetic defects in the mitochondrial (3243A > G, 10158T > C, 4.7 kb mtDNA deletion) or nuclear (*FRDA*, *POLG1*, *SURF-1*) genomes. All patients, except Patient 8 (Pearson syndrome) in whom neurological examination was

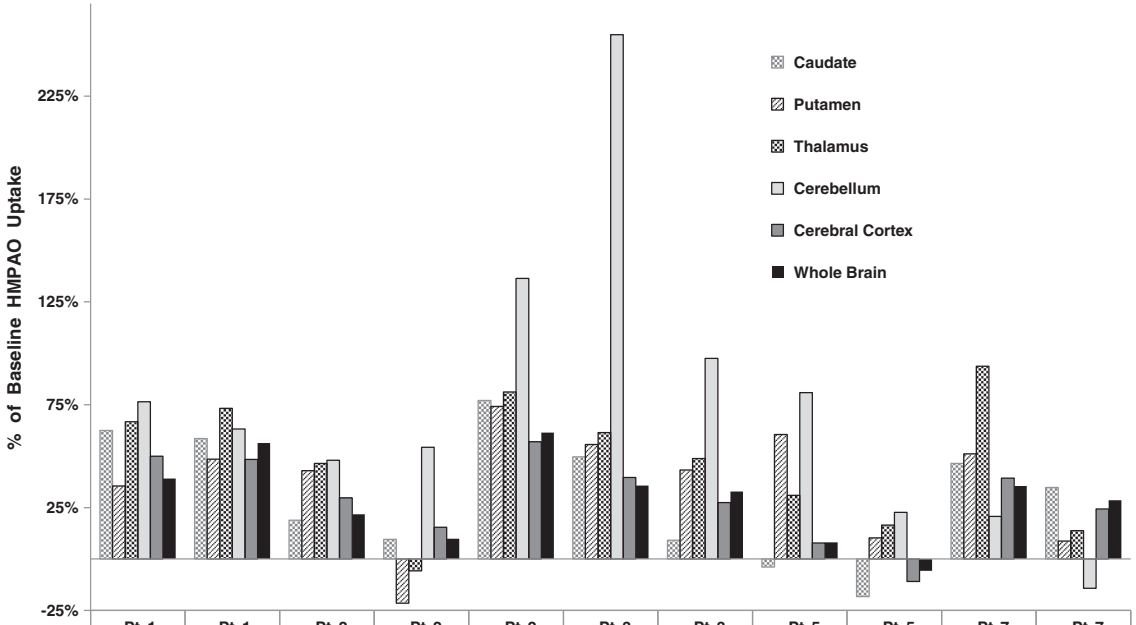

	Pt-1 3 Months	Pt-1 12 Months	Pt-2 3 Months	Pt-2 5 Months	Pt-2 12 Months	Pt-3 3 Months	Pt-3 10 Months	Pt-5 3 Months	Pt-5 4 Months	Pt-7 3 Months	Pt-7 5 Months
Caudate	62%	59%	19%	10%	77%	50%	9%	-4%	-18%	47%	35%
Putamen	36%	49%	43%	-21%	74%	56%	43%	61%	10%	51%	9%
Thalamus	67%	73%	46%	-6%	81%	61%	49%	31%	17%	94%	14%
Cerebellum	76%	63%	48%	54%	136%	255%	98%	81%	23%	21%	-14%
Cerebral Cortex	50%	48%	30%	15%	57%	40%	27%	8%	-11%	39%	24%
Whole Brain	39%	56%	22%	10%	61%	36%	33%	8%	-6%	35%	29%

Fig. 5. Longitudinal brain HMPAO SPECT results in patients 1 (Friedreich ataxia), 2 (polymerase γ deficiency), 3 (Kearns–Sayre syndrome), 5 (choreoathetosis, 3243A > G), and 7 (MELAS). HMPAO SPECT results compared to baseline at 3-months and most recent scan time points for Patients 1, 2, 3, 5, and 7 are shown. Patient 1 (Friedreich ataxia) demonstrated overall progressive improvement in HMPAO uptake from 3 to 12 months after starting EPI-743 therapy, with whole brain uptake increasing from 39% at 3-months to 56% at 12-months. Increased HMPAO uptake correlated with improved clinical status, including partial regaining of sight. Patient 2 (polymerase γ deficiency) showed initial improvement over the first 3 months of the treatment protocol, and then started to develop increasing weakness and spared cognitive ability, with correspondingly lower brain HMPAO uptake being noted at 5 months. Following an increase in dose of EPI-743 to maximal allowed by the protocol, HMPAO uptake increased at 12 months and her disease progression seemed to stabilize. Patient 3 showed improved clinical status at 3 months and 10 months, although the pace of improvement was greater during the first 3 months of therapy. Patient 5 (choreoathetosis, 3253A > G) had a greatly improved clinical status by 4 months following improved absorption of EPI-743, but brain HMPAO uptake was surprisingly lower. This may have been caused by increased metabolism, biliary excretion, or both of HMPAO secondary to starting high-dose phenobarbital [32]. Patient 7 (MELAS) improved over the 3-month protocol and then seemed to have a mild regression of speech ability after initial improved fluency, although motor skills were preserved. HMPAO uptake seemed to be lower especially in the cerebellum (see text and Supplemental Data for further details).

normal, exhibited a mitochondrial encephalomyopathy phenotype, and in addition manifested a variety of idiosyncratic clinical signs and symptoms also common to these diseases.

The clinical treatment course of the majority of patients was a departure from the natural history of end-stage inherited mitochondrial disease. All participants, except Patient 12 (polymerase γ deficiency), completed the initial 3-month protocol. Patient 12 was the most severely affected patient enrolled, had the highest NPMDS score, and also demonstrated the most rapid progression of disease. In addition, the thirteen patients who survived to complete the 3-month protocol exhibited objective and subjective signs of clinical improvement at least for a portion of the treatment protocol duration (Table 1, Supplemental Data). Patient 9 (Surf-1 deficiency) had been demonstrating clinical improvement after starting EPI-743 treatment, but died suddenly after developing respiratory failure secondary to severe brainstem disease 5 months after completion of the 3-month protocol. He was taking EPI-743 at the time of demise as part of an extension phase protocol.

In this study, we also evaluated the potential utility of brain HMPAO SPECT scanning to assess baseline redox disturbances and response to treatment. While brain MRI and MRS have been typically used to characterize these patient populations anatomically and functionally, such methods lack sensitivity to detect redox disturbances, and may also be latent in detecting changes. In 11 of 12 patients, HMPAO SPECT changes were sensitive and specific correlates to clinical status and treatment response. These data suggest that HMPAO SPECT imaging may be a valuable modality to measure redox disturbances that are a hallmark of mitochondrial and other diseases in both clinical and pre-clinical settings.

Patient 5 (choreoathetosis, 3243A > G) was the only participant to show discordance between clinical status and brain HMPAO uptake, demonstrating clinical improvement while the HMPAO uptake decreased. However, high-dose barbiturates are known to decrease brain HMPAO uptake and also stimulate biliary HMPAO excretion [30–32], which may explain this observation. Patient 5 was also found to have transient poor absorption of EPI-743 associated with a period of poor clinical status (persistent and increasing choreoathetosis). Following correction of an underlying enteropathy in the extension phase of the protocol, Patient 5 exhibited dramatic clinical improvement that correlated with normalization of drug absorption. Patient 8 (Pearson syndrome) also showed a fall in brain HMPAO uptake at 3 months, but her clinical status had worsened at the time of the brain scan following a hospitalization for treatment of pancreatitis, a urinary tract infection, and *Clostridium dificile* enterocolitis. In addition, her absorption of EPI-743 had fallen almost 60-fold when pharmacokinetic samples were obtained again after 6-months of

therapy, so it is possible that the low brain HMPAO uptake in this case was related decreased systemic EPI-743 levels.

HMPAO SPECT scanning appears to be a potential useful tool to judge *in vivo* brain redox status longitudinally given the apparent ability of this modality to detect alterations in redox status that appear to correlate to clinical status. Patient 2 is an illustration of this; initial improvement in strength and mobility was associated with increased HMPAO uptake, while decreased uptake was noted during a period of progression of disease. During a 2-month trial of a decreased dose of EPI-743, her disease seemed to progress at a more rapid rate and the dose of EPI-743 was then increased to the maximal allowed in this protocol. Following the increase in dose, she appeared to stabilize and this stabilization was accompanied by an increase in brain HMPAO uptake (Fig. 5). Although these initial results are interesting, longitudinal evaluation of more patients is clearly needed to determine the sensitivity of this technique for monitoring mitochondrial function.

The efficacy of EPI-743 in treating different subtypes of mitochondrial disease is still under investigation. It is possible that the variable response observed in Patient 2, as well as the death of Patient 12, are indications that polymerase γ deficiency may be relatively difficult to treat with a redox-modulating drug, but additional studies are needed to determine if mitochondrial disorders caused by different molecular defects respond variably to EPI-743. The severely affected patients described in this report serve as a sobering reminder about the difficulties children affected by mitochondrial disease face on a daily basis. Although EPI-743 stabilized clinical status and improved many aspects of daily life, as noted by the improvements in quality-of-life, several patients still experienced progression of some aspects of their underlying disorder. It is reasonable to speculate that mitochondrial disease patients with more mild symptoms and slower disease progression could experience an at least equal, and perhaps greater, benefit from treatment with EPI-743. It should be noted that the patients treated in this study were severely impaired and within 90 days of end-of-life care, with little hope of disease reversal or remission.

Although the precise mechanism of action of EPI-743 is under investigation, one mode of action being explored relates to its effect on cellular glutathione redox state. This hypothesized mechanism is supported by several observations: i) improved HMPAO uptake as seen by serial SPECT scanning with EPI-743 treatment; ii) cellular assays of glutathione depletion and EPI-743 rescue (Fig. 2); and iii) cellular data demonstrating normalization of antioxidant response element genes following EPI-743 treatment (Table 2). In addition, there is considerable precedent for alterations in brain glutathione metabolism in a variety of acute and chronic central nervous system diseases associated with oxidative stress [37–43]. Furthermore, targeting glutathione levels has recently been shown to be an effective therapeutic strategy in ethylmalonic encephalopathy, another disorder associated with mitochondrial dysfunction [44].

The current study has limitations inherent in the expanded-access nature of this protocol. In addition to using each subject as an internal control, there are significant challenges related to disease heterogeneity and pathogenesis. Furthermore, the emergency treatment protocol duration is relatively short; although all surviving patients have been enrolled in an ongoing extension protocol, it will be important to follow them over time to determine whether therapeutic gains are sustained. Finally, this study used a single dosing regimen that was followed according to FDA guidelines. All patients, regardless of age or weight, received the same EPI-743 dose, so some of the variability in response may be simply related to individual differences in drug concentration and bioavailability. As mentioned above, two patients had poor absorption of EPI-743, at least during part of the treatment period, which may have contributed to the lack of clinical response.

Despite these limitations, the data obtained in this study suggest that EPI-743 is safe and effective and may alter the natural history of mitochondrial disease progression. In addition, the tandem use of the novel redox therapeutic EPI-743 with the brain redox-imaging agent HMPAO may represent a new translational paradigm for the diagnosis, treatment and assessment of individuals with inherited mitochondrial disease and, therefore, merits further study. Prospective controlled trials will be undertaken to substantiate these initial promising observations.

Conflict of interest statement

Dr. Enns reports receiving unrestricted research funds from Edison Pharmaceuticals, Inc. Dr. Blankenberg is an imaging consultant for Edison Pharmaceuticals, Inc. Dr. Kinsman and Dr. Cohen report receiving funds for meeting travel from Edison Pharmaceuticals, Inc. Drs. Amagata, Barnes, Kheifets, Shrader, Thoolen, and Miller are employees of Edison Pharmaceuticals, Inc. Drs. Abdenur, Perlman, and Spicer report no disclosures.

Acknowledgments

The project described in this publication was supported by the Stanford NIH/NCRR CTSA award number UL1 RR025744 and by the Lucile Packard Foundation for Children's Health. The authors are grateful to the patients and their families, to Katherine Connors, MPH, Elizabeth Merkel, RN, Kelly Covault, RN, Deanna Fanning, RN, Andrea Frank, MSN, CPNP, and Hilary Wolf, RN for clinical trial coordination, Rachel Cox, MS, Julia Platt, MS, Deborah M. Alcorn, MD, Dorsey M. Bass, MD, Robin Casey, MD, Harvey J. Cohen, MD, PhD, Heidi Feldman, MD, PhD, Bertil E. Glader, MD, PhD, Kimberly Griesemer, CPNP, Jin S. Hahn, MD, Madelyn D. Kahana, MD, John M. Kerner, Jr., MD, Shawn Kile, MD, Joseph Kim, MD, Elliot J. Krane, MD, Christopher Longhurst, MD, Nathan Luna, MD, Carlos E. Milla, MD, Edward K. Neely, MD, Julie Reed, CPNP, Colin Roberts, MD, David N. Rosenthal, MD, Russell P. Saneto, DO, PhD, Laurie H. Seaver, MD, Barbara M. Sourkes, PhD, Lawrence Steinman, MD, Ching H. Wang, MD, PhD, Kiersten Wells, CPNP, Hsi-Yang Wu, MD, Nanci Yuan, MD, and William J. Zinnanti, MD, PhD for the clinical care provided to our patients, and Matthew Klein, M.D. for critical reading of the manuscript and help with statistical analysis.

Appendix A. Supplementary data

Supplementary data to this article can be found online at doi:10.1016/j.ymgme.2011.10.009.

References

[1] S. DiMauro, E.A. Schon, Mitochondrial respiratory-chain diseases, N. Engl. J. Med. 348 (2003) 2656–2668.
[2] A. Spinazzola, M. Zeviani, Mitochondrial diseases: a cross-talk between mitochondrial and nuclear genomes, Adv. Exp. Med. Biol. 652 (2009) 69–84.
[3] H.R. Elliott, D.C. Samuels, J.A. Eden, C.L. Relton, P.F. Chinnery, Pathogenic mitochondrial DNA mutations are common in the general population, Am. J. Hum. Genet. 83 (2008) 254–260.
[4] D.S. Kerr, Treatment of mitochondrial electron transport chain disorders: a review of clinical trials over the past decade, Mol. Genet. Metab. 99 (2010) 246–255.
[5] D.C. Wallace, Mitochondrial diseases in man and mouse, Science 283 (1999) 1482–1488.
[6] K.R. Atkuri, T.M. Cowan, T. Kwan, A. Ng, L.A. Herzenberg, G.M. Enns, Inherited disorders affecting mitochondrial function are associated with glutathione deficiency and hypocitrullinemia, Proc. Natl. Acad. Sci. U. S. A. 106 (2009) 3941–3945.
[7] I.P. Hargreaves, Y. Sheena, J.M. Land, S.J. Heales, Glutathione deficiency in patients with mitochondrial disease: implications for pathogenesis and treatment, J. Inherit. Metab. Dis. 28 (2005) 81–88.
[8] M.A. Tarnopolsky, The mitochondrial cocktail: rationale for combined nutraceutical therapy in mitochondrial cytopathies, Adv. Drug Deliv. Rev. 60 (2008) 1561–1567.
[9] R.T. Matthews, L. Yang, S. Browne, M. Baik, M.F. Beal, Coenzyme Q10 administration increases brain mitochondrial concentrations and exerts neuroprotective effects, Proc. Natl. Acad. Sci. U. S. A. 95 (1998) 8892–8897.
[10] C.W. Shults, R. Haas, Clinical trials of coenzyme Q10 in neurological disorders, Biofactors 25 (2005) 117–126.
[11] E.I. Glover, J. Martin, A. Maher, R.E. Thornhill, G.R. Moran, M.A. Tarnopolsky, A randomized trial of coenzyme Q10 in mitochondrial disorders, Muscle Nerve 42 (2010) 739–748.

[12] M. Stamelou, A. Reuss, U. Pilatus, J. Magerkurth, P. Niklowitz, K.M. Eggert, A. Krisp, T. Menke, C. Schade-Brittinger, W.H. Oertel, G.U. Hoglinger, Short-term effects of coenzyme Q10 in progressive supranuclear palsy: a randomized, placebo-controlled trial, Mov. Disord. 23 (2008) 942–949.
[13] R.S. Chen, C.C. Huang, N.S. Chu, Coenzyme Q10 treatment in mitochondrial encephalomyopathies. Short-term double-blind, crossover study, Eur. Neurol. 37 (1997) 212–218.
[14] Y. Ikejiri, E. Mori, K. Ishii, K. Nishimoto, M. Yasuda, M. Sasaki, Idebenone improves cerebral mitochondrial oxidative metabolism in a patient with MELAS, Neurology 47 (1996) 583–585.
[15] Y. Mashima, Y. Hiida, Y. Oguchi, Remission of Leber's hereditary optic neuropathy with idebenone, Lancet 340 (1992) 368–369.
[16] T. Klopstock, P. Yu-Wai-Man, K. Dimitriadis, J. Rouleau, S. Heck, M. Bailie, A. Atawan, S. Chattopadhyay, M. Schubert, A. Garip, M. Kernt, D. Petraki, C. Rummey, M. Leinonen, G. Metz, P.G. Griffiths, T. Meier, P.F. Chinnery, A randomized placebo-controlled trial of idebenone in Leber's hereditary optic neuropathy, Brain 134 (2011) 2677–2686.
[17] B.E. Drinkard, R.E. Keyser, S.M. Paul, R. Arena, J.F. Plehn, J.A. Yanovski, N.A. Di Prospero, Exercise capacity and idebenone intervention in children and adolescents with Friedreich ataxia, Arch. Phys. Med. Rehabil. 91 (2010) 1044–1050.
[18] D.R. Lynch, S.L. Perlman, T. Meier, A phase 3, double-blind, placebo-controlled trial of idebenone in Friedreich ataxia, Arch. Neurol. 67 (2010) 941–947.
[19] M.D. Esposti, A. Ngo, A. Ghelli, B. Benelli, V. Carelli, H. McLennan, A.W. Linnane, The interaction of Q analogs, particularly hydroxydecyl benzoquinone (idebenone), with the respiratory complexes of heart mitochondria, Arch. Biochem. Biophys. 330 (1996) 395–400.
[20] W.D. Shrader, A. Amagata, A. Barnes, G.M. Enns, A. Hinman, O. Jankowski, V. Kheifets, R. Komatsuzaki, E. Lee, P. Mollard, K. Murase, A.A. Sadun, M. Thoolen, K. Wesson, G. Miller, alpha-Tocotrienol quinone modulates oxidative stress response and the biochemistry of aging, Bioorg. Med. Chem. Lett. 21 (2011) 3693–3698.
[21] M.R. Jacquier-Sarlin, B.S. Polla, D.O. Slosman, Oxido-reductive state: the major determinant for cellular retention of technetium-99m-HMPAO, J. Nucl. Med. 37 (1996) 1413–1416.
[22] C. Phoenix, A.M. Schaefer, J.L. Elson, E. Morava, M. Bugiani, G. Uziel, J.A. Smeitink, D.M. Turnbull, R. McFarland, A scale to monitor progression and treatment of mitochondrial disease in children, Neuromuscul. Disord. 16 (2006) 814–820.
[23] A.M. Schaefer, C. Phoenix, J.L. Elson, R. McFarland, P.F. Chinnery, D.M. Turnbull, Mitochondrial disease in adults: a scale to monitor progression and treatment, Neurology 66 (2006) 1932–1934.
[24] T. Sasaki, M. Senda, Technetium-99m-meso-HMPAO as a potential agent to image cerebral glutathione content, J. Nucl. Med. 38 (1997) 1125–1129.
[25] S.J. Colloby, J.D. Fenwick, E.D. Williams, S.M. Paling, K. Lobotesis, C. Ballard, I. McKeith, J.T. O'Brien, A comparison of (99m)Tc-HMPAO SPET changes in dementia with Lewy bodies and Alzheimer's disease using statistical parametric mapping, Eur. J. Nucl. Med. Mol. Imaging 29 (2002) 615–622.
[26] J. Talairach, P. Tournoux, Co-planar Sterotaxic Atlas of the Human Brain: 3-Dimensional Proportional System—An Approach to Cerebral Imaging, Thieme Medical Publishers, New York, 1988.
[27] E. Suess, S. Malessa, K. Ungersbock, P. Kitz, I. Podreka, K. Heimberger, O. Hornykiewicz, L. Deecke, Technetium-99m-d,1-hexamethylpropyleneamine oxime (HMPAO) uptake and glutathione content in brain tumors, J. Nucl. Med. 32 (1991) 1675–1681.
[28] S. Zerarka, L. Pellerin, D. Slosman, P.J. Magistretti, Astrocytes as a predominant cellular site of (99m)Tc-HMPAO retention, J. Cereb. Blood Flow Metab. 21 (2001) 456–468.
[29] S.S. Chan, W.C. Copeland, DNA polymerase gamma and mitochondrial disease: understanding the consequence of POLG mutations, Biochim. Biophys. Acta 1787 (2009) 312–319.
[30] W.A. Volkert, T.J. Hoffman, R.M. Seger, D.E. Troutner, R.A. Holmes, 99mTc-propylene amine oxime (99mTc-PnAO); a potential brain radiopharmaceutical, Eur. J. Nucl. Med. 9 (1984) 511–516.
[31] R.D. Neirinckx, L.R. Canning, I.M. Piper, D.P. Nowotnik, R.D. Pickett, R.A. Holmes, W.A. Volkert, A.M. Forster, P.S. Weisner, J.A. Marriott, et al., Technetium-99m d, l-HM-PAO: a new radiopharmaceutical for SPECT imaging of regional cerebral blood perfusion, J. Nucl. Med. 28 (1987) 191–202.
[32] Y. Kamijo, K. Soma, R. Kondo, T. Ohwada, Transient diffuse cerebral hypoperfusion in Tc-99m HMPAO SPECT of the brain during withdrawal syndrome following acute barbiturate poisoning, Vet. Hum. Toxicol. 44 (2002) 348–350.
[33] M.E. Haffner, J. Whitley, M. Moses, Two decades of orphan product development, Nat. Rev. Drug Discov. 1 (2002) 821–825.
[34] A.M. Schaefer, R.W. Taylor, D.M. Turnbull, P.F. Chinnery, The epidemiology of mitochondrial disorders—past, present and future, Biochim. Biophys. Acta 1659 (2004) 115–120.
[35] J. Vockley, C.M. Vockley, Clinical trials: curing a critical deficiency in metabolic medicine, Mol. Genet. Metab. 99 (2010) 244–245.
[36] H.E. Heemstra, S. van Weely, H.A. Buller, H.G. Leufkens, R.L. de Vrueh, Translation of rare disease research into orphan drug development: disease matters, Drug Discov. Today 14 (2009) 1166–1173.
[37] J. Martensson, J.C. Lai, A. Meister, High-affinity transport of glutathione is part of a multicomponent system essential for mitochondrial function, Proc. Natl. Acad. Sci. U. S. A. 87 (1990) 7185–7189.
[38] A. Jain, J. Martensson, E. Stole, P.A. Auld, A. Meister, Glutathione deficiency leads to mitochondrial damage in brain, Proc. Natl. Acad. Sci. U. S. A. 88 (1991) 1913–1917.
[39] J. Sian, D.T. Dexter, A.J. Lees, S. Daniel, Y. Agid, F. Javoy-Agid, P. Jenner, C.D. Marsden, Alterations in glutathione levels in Parkinson's disease and other neurodegenerative disorders affecting basal ganglia, Ann. Neurol. 36 (1994) 348–355.
[40] S.J. Heales, S.E. Davies, T.E. Bates, J.B. Clark, Depletion of brain glutathione is accompanied by impaired mitochondrial function and decreased N-acetyl aspartate concentration, Neurochem. Res. 20 (1995) 31–38.
[41] J.E. Barker, J.P. Bolanos, J.M. Land, J.B. Clark, S.J. Heales, Glutathione protects astrocytes from peroxynitrite-mediated mitochondrial damage: implications for neuronal/astrocytic trafficking and neurodegeneration, Dev. Neurosci. 18 (1996) 391–396.
[42] R. Dringen, Glutathione metabolism and oxidative stress in neurodegeneration, Eur. J. Biochem. 267 (2000) 4903.
[43] S.J. Heales, J.P. Bolanos, Impairment of brain mitochondrial function by reactive nitrogen species: the role of glutathione in dictating susceptibility, Neurochem. Int. 40 (2002) 469–474.
[44] C. Viscomi, A.B. Burlina, I. Dweikat, M. Savoiardo, C. Lamperti, T. Hildebrandt, V. Tiranti, M. Zeviani, Combined treatment with oral metronidazole and N-acetylcysteine is effective in ethylmalonic encephalopathy, Nat. Med. 16 (2010) 869–871.